Adv Comput Math (2021) 47:74
https://doi.org/10.1007/s10444-021-09900-8

A rational RBF interpolation with conditionally positive definite kernels

Elham Farazandeh[1] · **Davoud Mirzaei**[1,2]

Received: 19 March 2021 / Accepted: 31 August 2021 / Published online: 27 September 2021

Abstract

In this paper, we present a rational RBF interpolation method to approximate multivariate functions with poles or other singularities on or near the domain of approximation. The method is based on scattered point layouts and is flexible with respect to the geometry of the problem's domain. Despite the existing rational RBF-based techniques, the new method allows the use of conditionally positive definite kernels as basis functions. In particular, we use polyharmonic kernels and prove that the rational polyharmonic interpolation is scalable. The scaling property results in a stable algorithm provided that the method be implemented in a localized form. To this aim, we combine the rational polyharmonic interpolation with the partition of unity method. Sufficient number of numerical examples in one, two and three dimensions are given to show the efficiency and the accuracy of the method.

Keywords Rational interpolation · Radial basis functions · Polyharmonic splines · Scalable approximations

Mathematics Subject Classification (2010) 41Axx · 65Nxx · 65Dxx

Communicated by: Robert Schaback

✉ Davoud Mirzaei
d.mirzaei@sci.ui.ac.ir

Elham Farazandeh
e.farazande@sci.ui.ac.ir

[1] Department of Applied Mathematics and Computer Science, Faculty of Mathematics and Statistics, University of Isfahan, 81746-73441, Isfahan, Iran

[2] School of Mathematics, Institute for Research in Fundamental Sciences (IPM), 19395-5746, Tehran, Iran

1 Introduction

Rational approximations are known to be much more effective than the standard (linear) ones for functions with poles or other singularities on or near the domain of approximation, or on unbounded domains. Univariate rational approximations with polynomials have a long history, but some new robust algorithms are recently being developed [10, 17, 21]. However, not much research has been devoted to multivariate rational approximations. In recent decades, the *radial basis function* (RBF) approximation has evolved into an excellent tool for solving multidimensional problems [4, 9, 23]. It is natural to ask for a multivariate rational RBF approximation for functions with steep gradients and/or singularities. In this direction, the first RBF-based rational interpolation algorithm was introduced in [14] with an application to approximation of antenna data. Then, a combination of this rational method with partition of unity (PU) approximation and a use of variably scaled kernels (VSK) [3] were done in [8] to improve the performance of the method. In [19] an application to discontinuous and steep gradient functions was provided, and in [5] the so-called eigen-rational kernel-based scheme was proposed which consists of a fractional RBF expansion with a denominator depending on the eigenvector associated to the largest eigenvalue of the kernel matrix.

The poles and singularities may be well captured if polynomial terms are appended to RBF expansions in numerator and denominator. Thus, conditionally positive definite kernels with respect to polynomial spaces, such as *polyharmonic splines*, should play an important role to enrich the available rational RBF approximations. However, the proposed rational RBF method in [14] (and then in [8, 19]) has some limitations in using conditionally positive definite kernels, which will be addressed in Section 2 after a brief review of the method. In this paper, a reformulation of the rational method for conditionally positive definite kernels is given which avoids those limitations and allows to implement the rational polyharmonic-based algorithm on *scaled data* to prevent the instability of the involved RBF systems. Following [8], the new rational interpolation is combined with the PU method by introducing some new simple weight functions. However, the main difference between the work of [8] and the present work addresses the rational part where the former uses the formulation of [14] for (strictly) positive definite kernels in a VSK setting while the later (the present work) focuses on conditionally positive definite kernels. Note that the rational interpolation of [5] allows the conditionally positive definite kernels as well, albeit in another formulation.

Here, we review the standard RBF interpolation. Assume that a conditionally positive definite function ϕ of order $m+1$ (with respect to polynomial space $\mathbb{P}_m^d$) is given. The RBF interpolation of a function $f : \Omega \to \mathbb{R}$ on a discrete set $X = \{x_1, \ldots, x_N\} \subset \Omega$ is given by

$$s_{f,X}(x) = \sum_{j=1}^{N} \alpha_j \phi(x - x_j) + \sum_{n=1}^{Q} a_n \ell_n(x) \tag{1}$$

where $\{\ell_1, \ldots, \ell_Q\}$ is a basis for $\mathbb{P}_m^d$, and $\boldsymbol{\alpha} = (\alpha_1, \ldots, \alpha_N)^T$ and $\boldsymbol{a} = (a_1, \ldots, a_Q)^T$ satisfy

$$\begin{bmatrix} K & P \\ P^T & 0 \end{bmatrix} \begin{bmatrix} \boldsymbol{\alpha} \\ \boldsymbol{a} \end{bmatrix} = \begin{bmatrix} \boldsymbol{f} \\ 0 \end{bmatrix}$$

where

$$\begin{aligned} K &= (\phi(x_j - x_k)) \in \mathbb{R}^{N\times N}, \\ P &= (\ell_n(x_j)) \in \mathbb{R}^{N\times Q}, \\ \boldsymbol{f} &= (f(x_1), \ldots, f(x_N))^T \in \mathbb{R}^N. \end{aligned}$$

We also need to assume $N \geqslant Q$ and X is $\mathbb{P}_m^d$-unisolvent to have a full rank matrix P. On the other hand, since ϕ is conditionally positive definite of order $m+1$, the symmetric matrix K is positive definite on $\ker(P^T)$ as a subspace of $\mathbb{R}^N$. These all guarantee that the interpolation system is uniquely solvable. The interpolant $s_{f,X}$ can also be written in the Lagrange form as

$$s_{f,X}(x) = \sum_{j=1}^{N} u_j(x) f(x_j), \tag{2}$$

where $(u_1(x), \ldots, u_N(x))^T =: \boldsymbol{u}(x)$ satisfies

$$\begin{bmatrix} K & P \\ P^T & 0 \end{bmatrix} \begin{bmatrix} \boldsymbol{u}(x) \\ \boldsymbol{v}(x) \end{bmatrix} = \begin{bmatrix} \boldsymbol{\phi}(x) \\ \boldsymbol{\ell}(x) \end{bmatrix}, \tag{3}$$

for $\boldsymbol{\phi}(x) = (\phi(x - x_1), \ldots, \phi(x - x_N))^T$ and $\boldsymbol{\ell}(x) = [\ell_1(x), \ldots, \ell_Q(x)]^T$. The Lagrange functions possess the property $u_j(x_k) = \delta_{kj}$.

The above-mentioned RBF interpolation will be used to compute numerator and denominator of the rational RBF interpolation of the next section.

2 Rational RBF interpolation

The rational RBF interpolation method of this section is an improvement of the method given in [14] in order to enrich it for conditionally positive definite kernels.

Assume that a set of points $X = \{x_1, x_2, \ldots, x_N\} \subset \Omega$ and a function $f : \Omega \to \mathbb{R}$ are given, and we want to determine a rational interpolation

$$\sigma_{f,X}(x) = \frac{p(x)}{q(x)} = \frac{\sum_{j=1}^{N} \alpha_j \phi(x - x_j) + \sum_{n=1}^{Q} a_n \ell_n(x)}{\sum_{j=1}^{N} \beta_j \phi(x - x_j) + \sum_{n=1}^{Q} b_n \ell_n(x)}$$

of f such that $\sigma_{f,X}(x_k) = f(x_k)$ for all $x_k \in X$. We assume that f, at least, is defined on set X. This problem has $2(N+Q)$ unknowns while N interpolation conditions, giving a flexibility to impose extra conditions on p and q. In [14] a condition is imposed on the native space semi-norms of p and q to be as small as possible relative to the size of their values at the data points to obtain sufficient smooth numerator and denominator functions. To give a precise formulation, assume that $\boldsymbol{p} = (p(x_1), \ldots, p(x_N))^T$, $\boldsymbol{q} = (q(x_1), \ldots, q(x_N))^T$, and $\|\boldsymbol{p}\|_2$ denotes the

2-norm of vector $\boldsymbol{p}$ in $\mathbb{R}^N$. Then, [14] suggests the following minimization problem to determine the rational interpolation:

$$\min \left\{ a|p|^2_{\mathcal{N}_\phi} + b|q|^2_{\mathcal{N}_\phi} : p, q \in \mathcal{N}_\phi,\ p(x_k) = f(x_k)q(x_k),\ c\|\boldsymbol{p}\|_2^2 + d\|\boldsymbol{q}\|_2^2 = 1 \right\}, \tag{4}$$

where a, b, c and d are four positive constants, $\mathcal{N}_\phi$ is the *native space* corresponding to the (conditionally) positive definite kernel ϕ, and $|\cdot|_{\mathcal{N}_\phi}$ is the usual (semi-) norm defined on this space. Of course, in the case of positive definite kernels, the semi-norm $|\cdot|_{\mathcal{N}_\phi}$ is replaced by the norm $\|\cdot\|_{\mathcal{N}_\phi}$. The minimizers p and q of the above problem determine the rational interpolant $\sigma_{f,X} = p/q$ of function f. In [14], by assuming the existence of the inverse matrix K^{-1}, the solution of the minimization problem (4) is recast to generalized eigenvalue problem $A\boldsymbol{q} = \lambda B\boldsymbol{q}$ where

$$\begin{aligned} A &= aDSD + bS, \\ B &= cD^2 + dI, \end{aligned}$$

in which $D = \mathrm{diag}\{f(x_1), \ldots, f(x_N)\}$, I is the identity matrix, and

$$S = K^{-1}\left(I - P\left(P^T K^{-1} P\right)^{-1} P^T K^{-1}\right).$$

Then the optimal vector $\boldsymbol{p}$ is given by $\boldsymbol{p} = D\boldsymbol{q}$, and the rational RBF interpolation is obtained by computing the standard RBF interpolations of nodal vectors $\boldsymbol{p}$ and $\boldsymbol{q}$.

This procedure works only for positive definite RBFs because the inverse of K may not exist for a conditionally positive definite function ϕ. Even if the inverse matrix exists for a special distribution of data points, the minimization problem (4) results in polynomial solutions p and q and neglects the radial parts in both numerator and denominator because the native space norm of a polynomial of degree at most m is necessarily zero.

In this paper, we improve the argument to fix these problems, and in particular we apply polyharmonic splines in order to benefit from their scalability property for a stable implementation. Apart from the rational interpolation, some parts of this section can be used to improve the exact expression of the standard RBF plus polynomial interpolation of [1] which is depending in the same way on existence of K^{-1}. First, we give some properties of the *saddle point* matrix

$$\begin{bmatrix} K & P \\ P^T & 0 \end{bmatrix} \tag{5}$$

where P has full rank and K is symmetric and positive definite on $\ker(P^T)$. For more details about saddle point matrices we refer the reader to [2] and the references therein.

Lemma 1 *If $P \in \mathbb{R}^{N\times Q}$ has full rank, $K \in \mathbb{R}^{N\times N}$ is symmetric and positive definite on $\ker(P^T)$ and $Z \in \mathbb{R}^{N\times(N-Q)}$ is any matrix whose columns form a basis for $\ker(P^T)$ then:*

(1) *The matrix $Z^T K Z$ is positive definite on $\mathbb{R}^{N-Q}$ and in particular it is invertible.*

(2) *The matrix*

$$Z(Z^T K Z)^{-1} Z^T =: S$$

is positive semi-definite on $\mathbb{R}^N$ *and positive definite on* $\ker(P^T)$.

(3) *The saddle point matrix* (5) *is invertible and its inverse is given by*

$$\begin{bmatrix} K & P \\ P^T & 0 \end{bmatrix}^{-1} = \begin{bmatrix} S & E \\ E^T & G \end{bmatrix}.$$

where $E = (I - SK)P(P^T P)^{-1}$ *and* $G = -(P^T P)^{-1} P^T K E$.

Proof The proof of (1) follows immediately from the fact that K is positive definite on $\ker(P^T)$. The proof of (2) follows from the fact that the left null space of Z (the null space of Z^T) is the orthogonal complement to the column space of Z. Item (3) can be verified by a direct computation, keeping in mind that $P^T P$ is invertible and $P(P^T P)^{-1} P^T = I - ZZ^T$. □

Item (2) of Lemma 5 shows that S has exactly Q zero and $N - Q$ non-zero eigenvalues because the dimension of $\ker(P^T)$ is $N - Q$. From here on, we assume that X is a $\mathbb{P}_m^d$-unisolvent set to have a full rank polynomial matrix P^T.

Lemma 2 *If* $s_{f,X}$ *is the standard interpolant of* f *on set* X *using a conditionally positive definite function* ϕ*, then its native space norm is given by*

$$|s_{f,X}|^2_{\mathcal{N}_\phi} = \boldsymbol{f}^T S \boldsymbol{f}$$

where $\boldsymbol{f} = (f(x_1), \ldots, f(x_N))^T$ *and* S *is defined in Lemma 1.*

Proof Since $s_{f,X}$ has the form (1), its semi-norm is given by $|s_{f,X}|^2_{\mathcal{N}_\phi} = \boldsymbol{\alpha}^T K \boldsymbol{\alpha}$ and since $s_{f,X}$ interpolates f, using Lemma 1 the coefficient vector $\boldsymbol{\alpha}$ satisfies $\boldsymbol{\alpha} = S\boldsymbol{f}$. This shows that $|s_{f,X}|^2_{\mathcal{N}_\phi} = \boldsymbol{f}^T SKS\boldsymbol{f}$. It is then straightforward to show that $SKS = S$ using the special representation of S. □

From Lemma 2 it is clear that if s is any function on the finite dimensional space $H_\phi(\Omega) \bigoplus \mathbb{P}_m^d$, where $H_\phi(\Omega)$ is the span of $\phi(\cdot - x_j)$ with coefficients α_j that satisfy $P^T \boldsymbol{\alpha} = 0$, then $|s|^2_{\mathcal{N}_\phi} = \boldsymbol{s}^T S \boldsymbol{s}$ where $\boldsymbol{s}$ is vector of $s(x_j)$ values.

In order to obtain a quadratic target function with a positive definite matrix, we replace the native space norms in the minimization problem (4) by

$$\|\cdot\|^2_{\mathcal{N}_\phi,X} := |\cdot|^2_{\mathcal{N}_\phi} + \gamma |\cdot|^2_X, \quad \gamma > 0, \tag{6}$$

where $|\cdot|_X$ is the discrete L_2 semi-norm on the $\mathbb{P}_m^d$-unisolvent set X. The above norm is induced by inner product

$$(f, g)_{\mathcal{N}_\phi,X} := (f, g)_{\mathcal{N}_\phi} + \gamma \sum_{k=1}^{N} f(x_k) g(x_k), \quad f, g \in \mathcal{N}_\phi.$$

Indeed, (6) defines a norm on $\mathcal{N}_\phi$ because $\|f\|_{\mathcal{N}_\phi,X} = 0$ implies that $|f|_{\mathcal{N}_\phi} = 0$ and $|f|_X = 0$, where the former gives $f \in \mathbb{P}_m^d$ which together with the later shows $f = 0$ because X is assumed to be a unisolvent set for $\mathbb{P}_m^d$. Later on, we shall use some special γ values to obtain an scalable numerical algorithm. Now, we define the new minimization problem

$$\min \left\{ a\|p\|^2_{\mathcal{N}_\phi,X} + b\|q\|^2_{\mathcal{N}_\phi,X} : p, q \in \mathcal{N}_\phi,\ \boldsymbol{p} = D\boldsymbol{q},\ c\|\boldsymbol{p}\|_2^2 + d\|\boldsymbol{q}\|_2^2 = 1 \right\}, \quad (7)$$

for positive constants a, b, c and d.

Theorem 1 *The solution of the minimization problem (7) is the least eigenvalue and the optimal solution $\boldsymbol{q}$ is the corresponding eigenvector to the generalized eigenvalue problem*

$$A\boldsymbol{q} = \lambda B\boldsymbol{q} \quad (8)$$

where

$$\begin{aligned} A &:= aD(S+\gamma I)D + b(S+\gamma I), \\ B &:= cD^2 + dI \end{aligned}$$

in which $D = \operatorname{diag}\{f(x_1), \ldots, f(x_N)\}$, I is the identity matrix, and S is defined in Lemma 1. The optimal vector $\boldsymbol{p}$ is given by $\boldsymbol{p} = D\boldsymbol{q}$. The rational RBF interpolation is obtained by $\sigma_{f,X} = p/q$ where p and q are the standard RBF interpolants of vectors $\boldsymbol{p}$ and $\boldsymbol{q}$, respectively.

Proof The proof of this theorem is the same as that of [14, Theorem 3.1]. According to Lemma 2 and norm definition (6), $\|q\|^2_{\mathcal{N}_\phi,X} = \boldsymbol{q}^T(S+\gamma I)\boldsymbol{q}$ and $\|p\|^2_{\mathcal{N}_\phi,X} = \boldsymbol{q}^T D(S+\gamma I)D\boldsymbol{q}$ because $\boldsymbol{p} = D\boldsymbol{q}$. Besides, it is clear that $c\|\boldsymbol{p}\|_2^2 + d\|\boldsymbol{q}\|_2^2 = \boldsymbol{q}^T(cD^2 + dI)\boldsymbol{q}$. Thus, the minimization problem (7) is identical with

$$\min \left\{ \boldsymbol{q}^T A\boldsymbol{q} :\ \boldsymbol{q}^T B\boldsymbol{q} = 1 \right\}.$$

In this formulation, $S+\gamma I$ is positive definite because S is positive semi-definite. Since we do not care about the f values, $D(S+\gamma I)D$ is (in general) positive semi-definite, but $A = aD(S+\gamma I)D + b(S+\gamma I)$ is necessarily positive definite, keeping in mind that a, b and γ are positive numbers. Moreover, B is a diagonal matrix with positive on-diagonal elements. It is obvious that the solution is the least eigenvector (corresponding to the least eigenvalue) of problem (8). □

In [19], the method of diagonal increments (MDI) is used to regularize the matrix K (obtained from the inverse multiquadric (IMQ) kernel) to remain numerically positive definite and to avoid the ill-conditioning. Then the matrix $K + \mu I$ is inverted instead of K where $\mu > 0$ is a small smoothing parameter. This regularization is different from our approach where γI is finally added to S, the counterpart of K^{-1} for positive definite kernels. Besides, γ may not be a small number, at all. To stabilize the algorithm for matrix inversions we will apply an efficient scaling technique. See Section 3.

In [14], some choices for constants a, b, c and d are discussed. In this paper we use $a = c = 1/\|\boldsymbol{f}\|_2$ and $b = d = 1$. This choice normalizes the two terms in definitions of both matrices A and B, and results in a homogeneous rational interpolation, i.e., $\sigma_{\alpha f,X} = \alpha\sigma_{f,X}$ for all real values α. See [14] for more details and other choices.

3 Polyharmonic kernels and scaling

Although all (conditionally) positive definite RBFs in the market [4, 9, 23] can be used, in this paper we employ the *polyharmonic* kernel

$$\varphi_\beta(r) := (-1)^{\lfloor \beta/2 \rfloor + 1} \times \begin{cases} r^\beta \log r, & \beta \text{ even} \\ r^\beta, & \text{otherwise} \end{cases} \tag{9}$$

for real number $\beta > 0$ and assume $\phi(x) = \varphi_\beta(\|x\|_2)$ for $x \in \mathbb{R}^d$. The polyharmonic kernel φ_β is conditionally positive definite of order $m + 1 = \lfloor \beta/2 \rfloor + 1$.

We are encouraged by the scalability property of polyharmonic kernels to use them in the rational interpolation algorithm. This property allows avoiding the instability of RBF systems. The rational interpolation of the previous section could be subdivided into two phases (i) forming and solving the eigenvalue problem (8) for nodal vector $\boldsymbol{q}$, and (ii) solving the standard RBF system (3) and using (2) to obtain the denominator q and the numerator p from nodal vectors $\boldsymbol{q}$ and $\boldsymbol{p} = D\boldsymbol{q}$, respectively. The scaling can be applied in both phases. Indeed, for the standard polyharmonic interpolation (the second phase) the scaling idea is not new and can be traced back to [11]. See also [7, 12, 13, 16] for applications to numerical solution of PDEs. After reviewing the scaling property for the standard interpolation, we will show that the scaling works in the first phase of the rational interpolation as well.

It is proved in [11] that the polyharmonic Lagrange functions u_j from (3) are invariant under the scaling. Let's describe this in more detail. Assume that X_h is a set of points in Ω with maximum pairwise distance h. Assume further that the polyharmonic interpolation (2) on X_h at a fixed evaluation point $x_h \in \Omega$ is sought. The kernel matrix K (as well as the interpolation matrix in (3)) becomes algebraically ill-conditioned as h decreases [23, chap. 12]. To fix this problem, we can divide (scale) the trial points X_h and the evaluation point x_h both by h to get a new blown-up set X of average pairwise distance 1 and a new evaluation point x. Let's denote the Lagrange functions on X_h by $u_{h,j}$. We can prove that Lagrange functions u_j obtained by solving (3) are identical with Lagrange functions of the original situation, i.e., $u_j(x) = u_{j,h}(x_h)$. See [11] for details. It is clear that in the blown-up situation the conditioning of (3) behaves as $\mathcal{O}(1)$. This scaling approach works much better if the RBF interpolation is implemented in a localized form. In this case, if the monomials $\{x^\mu\}_{|\mu| \leqslant m}$ are used as a basis for $\mathbb{P}_m^d$, then it is highly recommended to *shift* the points by the center of the local domain and then scale by h to benefit from the local behavior of the monomial basis functions around the origin. Note that, on behalf of the radial part, we are allowed to shift because our approximation space is shift (and rotation) invariant.

However, it is not the whole story and we can show further that the optimal solution $\boldsymbol{q}$ of the minimization problem (7), which is obtained from the generalized eigenvalue problem (8), is invariant under the scaling. In doing so, we recall [23, Proposition 8.4].

Proposition 1 *Every polynomial p of degree at most $2m+1$ is conditionally positive definite of order $m+1$. More precisely, for all N, all sets $X = \{x_1, \ldots, x_N\} \subset \mathbb{R}^d$ and all $\boldsymbol{\alpha} \in \mathbb{R}^N$ with $P^T\boldsymbol{\alpha} = 0$, the quadratic form $\boldsymbol{\alpha}^T \tilde{K}\boldsymbol{\alpha}$ is identically zero. Here $\tilde{K} = (p(x_k - x_j))$ for $k, j = 1, \ldots, N$.*

Theorem 2 *Let $h > 0$ be an arbitrary real number. The optimal solution $\boldsymbol{q}$ of the generalized eigenvalue problem (8) is invariant under h-scaling provided that the polyharmonic kernel (9) is used, and $\gamma = h^{-\beta}$ in (6).*

Proof Let X be a fixed set of points in Ω and K be the kernel interpolation matrix on X. Assume K_h and P_h are kernel and polynomial matrices on the scaled set $hX = \{hx_1, \ldots, hx_N\}$ for $h > 0$. Using this notation, $K_1 = K$ and $P_1 = P$. If the monomial basis $\{x^\alpha\}_{|\alpha| \leqslant m}$ is used for polynomial space $\mathbb{P}_m^d$ then $P_h = PH$ with

$$H = \operatorname{diag}\Big\{1, \underbrace{h, \ldots, h}_{\binom{d}{d-1} \text{ times}}, \underbrace{h^2, \ldots, h^2}_{\binom{d+1}{d-1} \text{ times}}, \ldots, \underbrace{h^m, \ldots, h^m}_{\binom{d+m-1}{d-1} \text{ times}}\Big\} \in \mathbb{R}^{Q \times Q},$$

keeping in mind that $\#\{x^\alpha : |\alpha| = k\} = \binom{d+k-1}{d-1}$ for $k = 0, 1, \ldots, m$. As H is a full rank diagonal matrix, we simply have $Z_h := \ker(P_h^T) = \ker(P^T) = Z$.

For power kernel $\varphi_\beta(r) = r^\beta$ it is clear that $K_h = h^\beta K$. Thus

$$S_h = Z_h \left(Z_h^T K_h Z_h\right)^{-1} Z_h^T = h^{-\beta} Z \left(Z^T K Z\right)^{-1} Z^T = h^{-\beta} S$$

and

$$A_h = aD(S_h + \gamma I)D + b(S_h + \gamma I) = h^{-\beta}(aD(S + I)D + b(S + I)) = h^{-\beta} A_1.$$

The diagonal matrix B in (8) is independent of h. These show that $\boldsymbol{q}_h = \boldsymbol{q}$ and $\lambda_h = h^{-\beta}\lambda$.

For thin plate spline $\varphi_\beta(r) = r^\beta \log r$, $\beta \in 2\mathbb{N}$, we have $\varphi_\beta(hr) = h^\beta \varphi_\beta(r) + h^\beta \log h\, r^\beta =: h^\beta \varphi_\beta(r) + p$ where p is a polynomial of degree at most β. According to Proposition 1, since $\varphi_\beta(\|\cdot\|_2)$ is conditionally positive definite of order $\beta/2 + 1$ and columns of Z form a basis for $\ker(P^T) = \ker(P_h^T)$ we have $Z^T \tilde{K} Z = 0$ where $\tilde{K}$ is the kernel matrix of polynomial $p \in \mathbb{P}_\beta(\mathbb{R}^d)$. By a direct computation, we again have $S_h = h^{-\beta} S$, $A_h = h^{-\beta} A_1$, $\boldsymbol{q}_h = \boldsymbol{q}$ and $\lambda_h = h^{-\beta}\lambda$. □

According to Theorem 2, for a set of interpolation points with fill distance h on a local domain $\mathcal{D}$, first we shift the points by the center of $\mathcal{D}$ and then divide them by h to get a new blown-up set around the origin. Then we only need to form

$$A = aD(S + I)D + b(S + I), \quad B = cD^2 + dI,$$

where S is constructed on the blown-up situation. The least eigenvector $\boldsymbol{q}$ of the eigenvalue problem $A\boldsymbol{q} = \lambda B\boldsymbol{q}$ and $\boldsymbol{p} = D\boldsymbol{q}$ give the nodal values of the denominator and the numerator, respectively. Finally, according to the discussions before Theorem 2, the standard RBF interpolants p and q can be similarly computed via the Lagrange functions on the blown-up situation.

It is important to note that the scaling strategy prevents the instability in two lines of the rational algorithm: (i) in computing the matrix S where $Z^T K^{-1} Z$ needs to be formed, and (ii) in computing the numerator p and the denominator q where the saddle point matrix (5) needs to be inverted. However, the scaling is computationally more efficient for local interpolation problems where h is decreased while the number of points in each local domain is fixed. To this aim, in the next section, we implement the rational RBF interpolation in a partition of unity setting.

4 Partition of unity rational interpolation

The global RBF approximations, standard or rational, suffer from the problem of producing full and ill-conditioned matrices. This makes them restricted for application on large scale problems, specially in multivariate cases. A possible solution to this problem is to implement them in a localized form, such as in combination with a partition of unity (PU) method [8, 22]. Here we use the rational polyharmonic interpolation of the preceding section in a PU setting to obtain a localized rational RBF method. We also introduce a new constant-generated PU weight that simplifies the computations regarded to the PU approximation. In local patches we use the scaled polyharmonic interpolation (Section 3) to stabilize the local systems.

Let $\{\Omega_\ell\}_{\ell=1}^{N_c}$ be an open and bounded covering of $\Omega \subset \mathbb{R}^d$ that means all Ω_ℓ are open and bounded and $\Omega \subset \bigcup_{\ell=1}^{N_c} \Omega_\ell$. This grantees that every point $x \in \Omega$ is necessarily covered by at least one patch Ω_ℓ. A family of nonnegative functions $\{w_\ell\}_{\ell=1}^{N_c}$ is called a partition of unity with respect to the covering $\{\Omega_\ell\}$ if

(1) $\operatorname{supp}(w_\ell) \subseteq \Omega_\ell$,

(2) $\displaystyle\sum_{\ell=1}^{N_c} w_\ell(x) = 1, \ \forall x \in \Omega.$

We start with an overlapping covering $\{\Omega_\ell\}_{\ell=1}^{N_c}$ of Ω. If σ_ℓ are local rational RBF interpolations of function u on discrete sets $X_\ell \subset \Omega_\ell$, then it is clear that

$$\sigma = \sum_{\ell=1}^{N_c} w_\ell \sigma_\ell \tag{10}$$

is a global interpolation of u on $X = \bigcup_{\ell=1}^{N_c} X_\ell \subset \Omega$. A possible choice for w_ℓ is the Shepard's weights [20]

$$w_\ell(x) = \frac{\psi_\ell(x)}{\sum_{j=1}^{N_c} \psi_j(x)}, \quad 1 \leqslant \ell \leqslant N_c, \tag{11}$$

where ψ_ℓ are nonnegative, nonvanishing and compactly supported functions on Ω_ℓ.

The PU approach allows to compute small rational RBF interpolants on patches Ω_ℓ, and then join them by PU weights to form a global rational approximation on the whole Ω. This leads to a computationally more efficient algorithm which avoids handling a single but very large system in favor of solving several small systems.

A simple covering for Ω can be constructed via a set of overlapped balls $\Omega_\ell = B(\omega_\ell, \rho_\ell)$ where $\omega_\ell \in \mathbb{R}^d$ are patch centers and ρ_ℓ are patch radii. We use the following setup for points, parameters and domain sizes for the rational RBF-PU interpolation algorithm. We assume that $X = \{x_1, \ldots, x_N\}$ is a set of interpolation points in Ω with *fill distance*

$$h = h_{X,\Omega} = \max_{x\in\Omega} \min_{x_k\in X} \|x - x_k\|_2.$$

The fill distance indicates how well the points in the set X fill out the domain Ω. Geometrically, h is the radius of the largest possible empty ball that can be placed among the data locations X inside Ω. A grid point set $\{\omega_1, \ldots, \omega_{N_c}\}$ with space distance

$$h_{\text{cov}} = C_{\text{cov}} h, \quad C_{\text{cov}} > 1 \tag{12}$$

is used for patch centers. The constant C_{cov} controls the number of patches compared with the number of interpolation points. If points in X are distributed quasi-uniformly then $N_c \approx N/C_{\text{cov}}^d$ because in this case $h \approx N^{-1/d}$. The radii ρ_ℓ control the amount of covering's overlap. Although light overlaps result in a faster algorithm, these radii should be large enough to guarantee the inclusion $\Omega \subset \cup B(\omega_\ell, \rho_\ell)$ and to allow enough trial points in each patch for a well-defined and accurate local interpolation. Thus, we let

$$\rho_\ell = C_{\text{ovlp}} h_{\text{cov}}, \quad C_{\text{ovlp}} > \sqrt{d}/2, \tag{13}$$

and we assume the overlap constant C_{ovlp} is large enough to ensure the above requirements. We may use larger C_{ovlp} for one-sided patches whose centers are close to the boundary of Ω. The settings (12) and (13) for the space distance between covering centers and radius of patches allow to have a *local* and *regular* covering $\{\Omega_\ell\}$ with respect to set X. Note that for a given set $X \subset \Omega$ a covering $\{\Omega_\ell\}$ is called local with respect to X if there exists a global constant C such that $\text{diam}(\Omega_\ell) \leqslant C h_{X,\Omega}$. And the covering is called regular if there exists a global constant L such that every $x \in \Omega$ is covered by at most L patches. The performance of a PU method is highly increased if the underlying covering is both local and regular [23, chap. 15].

To define a Shepard weight on $B(\omega_\ell, \rho_\ell)$, we assume that $\varphi : \mathbb{R}_{\geqslant 0} \to \mathbb{R}_{\geqslant 0}$ is a compactly supported function with a support on $[0, 1]$, and we define $\psi_\ell(x) = \varphi(\|x\|_2/\rho_\ell)$ in (11). As an example, the C^2 Wendland's function $\varphi(r) = (1 - r)_+^4(4r + 1)$ can be used that leads to a set of smooth PU weights $w_\ell \in C^2(\Omega)$. Such smooth weight functions are frequently used in PU approximations; see for example [6, 15, 18, 22]. Some discontinuous PU weights are also suggested in [16] that highly simplify the RBF-PU algorithms for solving partial differential equations. Of course, they can be implemented for pure interpolation as well. The simplest one which is introduced in the following is applied for numerical results of this paper. Let

$$I_{\min}(x) = \arg\min_{\ell\in I(x)} \|x - \omega_\ell\|_2$$

and $I_{\min,1}(x)$ be the first component of $I_{\min}(x)$, as $I_{\min}(x)$ may contain more than one index ℓ. The PU weight function is then defined by

$$w_\ell(x) := \begin{cases} 1, & \ell = I_{\min,1}(x) \\ 0, & \text{otherwise.} \end{cases} \tag{14}$$

With this definition, we give the total weight 1 to the closest patch to x and null weights to other patches. In fact, a local set $X_\ell = \Omega_\ell \cap X$ is a common trial set for all evaluation points x with $\|x - \omega_\ell\|_2 \leq \|x - \omega_j\|_2$ for $j = 1, \ldots, N_c$ and $j \neq \ell$.

Following the analysis of PU methods for standard interpolation [23], if in each region $\Omega_\ell \cap \Omega$, f is approximated by a rational function σ_ℓ such that

$$\|f - \sigma_\ell\|_{L_\infty(\Omega_\ell \cap \Omega)} \leqslant \varepsilon_\ell,$$

then the global rational interpolation σ satisfies

$$\begin{aligned} |f(x) - \sigma(x)| &\leqslant \sum_{\ell \in I(x)} w_\ell(x) \big| f(x) - \sigma_\ell(x) \big| \\ &\leqslant \sum_{\ell \in I(x)} w_\ell(x) \big\| f - \sigma_\ell \big\|_{L_\infty(\Omega_\ell \cap \Omega)} \\ &\leqslant \sum_{\ell \in I(x)} w_\ell(x) \varepsilon_\ell \\ &\leqslant \max_{\ell \in I(x)} \varepsilon_\ell, \end{aligned}$$

which means that the rational partition of unity interpolation is at least as good as its worst local interpolation. We note that the only property that is used is the partition of unity property. Thus, the above bound holds also true for discontinuous PU weights. Unfortunately, a theoretical estimation for local errors ε_ℓ is not straightforward and is left for a future study. Instead, we report experimental orders in our numerical tests in Section 5.

4.1 Computational cost

The computational complexity of the method includes the costs of solving local eigenvalue problems and local standard RBF interpolations in all patches. To estimate the number of points in each patch, we use a packing argument similar to that given in [23, chap. 4]. First, we define the *separation distance*

$$q_X := \frac{1}{2} \min_{j \neq k} \|x_j - x_k\|_2$$

of trial set X. The separation distance measures how well the points are disjoint from each others. In fact, q_X is the radius of the largest ball that can be placed around every point in X such that no two balls overlap. A set X is said to be *quasi-uniform* with respect to a constant c_{qu} if

$$q_X \leqslant h_{X,\Omega} \leqslant c_{\text{qu}} q_X. \tag{15}$$

The first inequality is obvious from definitions. Quasi-uniformity is not a property of a single set X but a sequence of such sets that gradually fill out the domain Ω. Then, (15) should be satisfied by all sets in this sequence with the same constant c_{qu}.

We assume that the sequence of our node refinements satisfies the quasi-uniformity property. Let $n_\ell = \#X_\ell$, the number of points in $\Omega_\ell = B(\omega_\ell, \rho_\ell)$. We simply have

$$n_\ell \times \mathrm{vol}\big(B(0, q_X)\big) \leqslant \mathrm{vol}\big(B(\omega_j, \rho_\ell + q_X)\big)$$

which gives

$$n_\ell c_d q_X^d \leqslant c_d(\rho_\ell + q_X)^d = c_d(C_{\mathrm{ovlp}} C_{\mathrm{cov}} h_{X,\Omega} + q_X)^d$$

where c_d is the volume of the unit ball in $\mathbb{R}^d$. The inequality $h_{X,\Omega} \leqslant c_{\mathrm{qu}} q_X$ then gives

$$n_\ell \leqslant (C_{\mathrm{ovlp}} C_{\mathrm{cov}} c_{\mathrm{qu}} + 1)^d =: n_L,$$

where n_L is a constant independent of the fill and separation distances (and thus independent of N), showing that the number of points in each patch remains unchanged, approximately, when the discretization is refined. Assume that the set of indices J_ℓ of interpolation points in Ω_ℓ is known in advance. The computational cost for forming and solving the eigenvalue problem (8) for the least eigenvalue is at most of order n_ℓ^3 and for solving the standard RBF interpolation is of order $(n_\ell + Q)^3$. Since n_ℓ is bounded by constant n_L the total cost for all patches is dominated by $N_c \mathcal{O}(n_L^3 + Q^3)$, where N_c is the number of patches. Since $N_c \approx N/C_{\mathrm{cov}}^d$, the computational cost is of order N where N is the number of interpolation points. This complexity analysis ignores the costs of collecting the indices of points in Ω_ℓ among all N interpolation points in X. But this can be done in a preprocessing step using a boxing strategy to avoid collecting J_ℓ for each patch center separately. By dividing the domain Ω into boxes of side length $\mathcal{O}(N^{-1/d})$ and collecting for each box the points that it contains the overall complexity would be $\mathcal{O}(N + N_c)$. As a more relevant strategy we can use a kd-tree algorithm that takes $\mathcal{O}(N \log N)$ time for building the tree on X and $\mathcal{O}(N^{1-1/d})$ time for range searchings. More details can be found in [23, chap. 14]. The complexity of evaluating the interpolant at a set X_e is dominated by the cost of building another data structure on X_e to collect the indices of evaluation points in each patch Ω_ℓ.

5 Numerical results

In this section some 1D, 2D and 3D experiments are given. In all cases we assume that $h = \mathcal{O}(N^{-1/d})$ is approximately the fill distance of interpolation points in X. For a given function f and a set X, if f is not defined on a point $x_k \in X$, we simply take this point out and work with $X \setminus \{x_k\}$ instead of X. We further assume that the set of patch centers has vertical (horizontal) mesh distance $h_{\mathrm{cov}} = 4h$ for 1D and 2D, and $h_{\mathrm{cov}} = 3h$ for 3D examples. We also use $C_{\mathrm{ovlp}} = 1$ to have $\rho_\ell = 4h$ (in 1D and 2D) and $\rho_\ell = 3h$ (in 3D) for patch radii, but we increase the radius of patches on or near the boundary of Ω by a factor of 1.5 (in 1D and 2D) and 1.3 (in 3D) to have enough interpolation points in those one-sided patches. These local sizes allow much more than Q interpolation points in local domains (≈ 9 in 1D, 45 in 2D, and 120 in 3D) to guarantee both unisolvency and high accuracy of local approximants. In all experiments we use the constant-generated PU weight function (14). Regular (grid) and Halton points are used in all numerical simulations. These settings are used

for both standard and rational interpolations. In all examples, the relative errors are measured in the discrete L_2 norm on a fine set of regular evaluation points which does not contain the singularities of the underlying function. In the legend of some figures by "Rational-Regular" we mean the rational RBF interpolation method on regular interpolation points, by "Rational-Halton" we mean the rational RBF interpolation on Halton points, and the same for "Standard-Regular" and "Standard-Halton." All convergence plots are on a log-log scale. Numerical convergence orders are obtained by the linear least squares fitting to error values and are written alongside the figure legends.

The algorithm is implemented in MATLAB and executed on a machine with an Intel Core i7 processor, 2.4.00 GHz, and 8 GB RAM. We also provide the MATLAB code, freely available at

https://github.com/ddmirzaei/Rational_RBF

to facilitate the reproduction of the examples presented.

As a smooth 1D example we consider

$$f(x) = \frac{1}{2 + \cos(20x + 1)}, \quad x \in [-1, 1],$$

and as a function with singularities we consider

$$f(x) = \frac{1}{J_0(x)}, \quad x \in [0, 20],$$

where J_0 is the order zero Bessel function of the first kind. The plots of these functions are shown in Fig. 1. The second function has six singularity points in [0, 20]. In Fig. 2 a comparison between the relative errors of the standard and the rational RBF interpolations via $\varphi(r) = r^3$ with linear polynomials is shown for both functions. For the smooth function, the theoretical order $m + 1 = 2$ is realized for the standard method and better numerical orders are obtained for the rational method. However, in this case the rational interpolation does not remarkably outperform the standard one, while for the function with singularities the rational interpolation is substantially more accurate, as expected. The rational algorithm works well with both regular and scattered interpolation points.

As another 1D example, we consider the function

$$f(x) = \frac{x}{\cos^3(\pi^2/3x)}, \quad x \in [-1, 1],$$

which has two singularities of order 3 in $[-1, 1]$. We again use the radial function r^3 but we augment polynomials of higher degrees to examine the role of polynomials to capture higher order poles. The results on regular and Halton points are shown in Fig. 3. Although the convergence is observed for $m = 1, 2$ (at larger values of N), an absolutely faster convergence is achieved when polynomials of degree 3 are appended.

Up to here, we did our experiments on some 1D functions that could also be treated by recent robust rational algorithms such as AAA [17], efficiently. However, it is known that the RBF approximations are more efficient for handling multidimensional

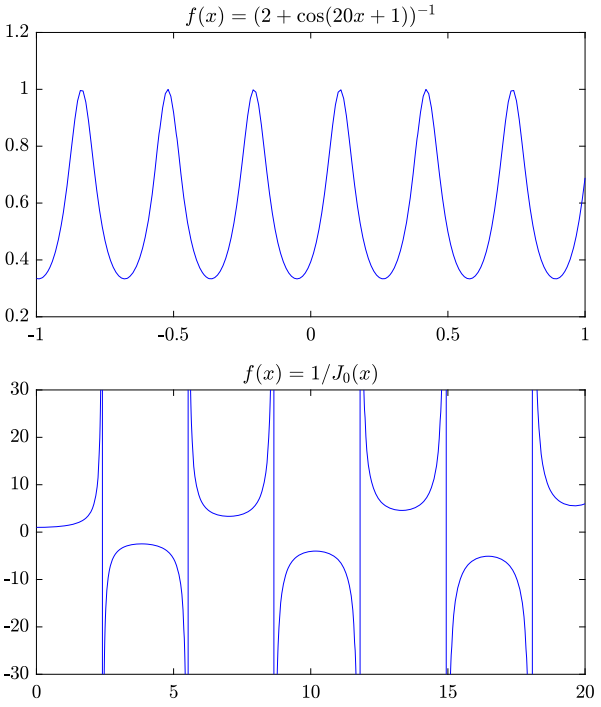

Fig. 1 Plots of 1D functions: a smooth function on interval $[-1, 1]$ (top) and a function with six singularities on $[0, 20]$ (bottom)

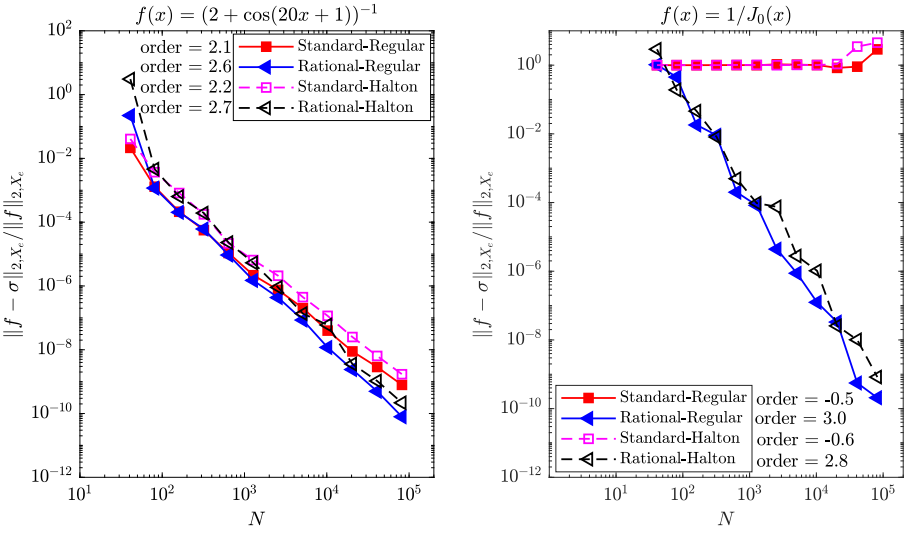

Fig. 2 Error plots for a smooth 1D function (left) and for a singular 1D function (right). Both standard and rational methods with regular and Halton interpolation points are implemented. The polyharmonic spline r^3 with polynomials of degree 1 is used

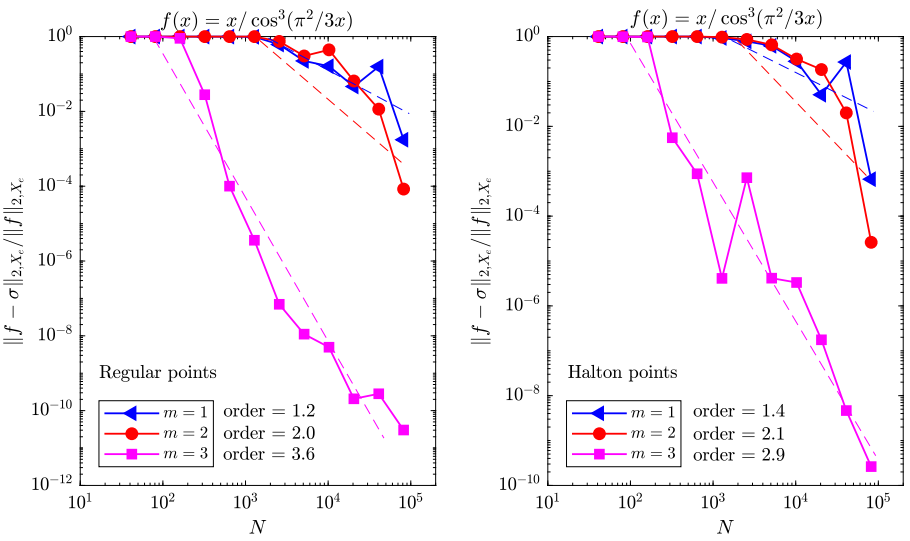

Fig. 3 Error plots for rational interpolation on regular and Halton points for a 1D function with high-order poles. The polyharmonic spline r^3 with polynomials of degrees $m = 1, 2, 3$ is used

problems where some available algorithms are not applicable. Here, some 2D and 3D examples are given. As a smooth bivariate function with a steep gradient, we assume

$$f(x, y) = \tan^{-1}\left(125\left(\sqrt{(x-1.5)^2 + (y-0.25)^2} - 0.92\right)\right), \quad (x, y) \in [0, 1]^2, \tag{16}$$

which has a steep wave front located asymmetrically in the unit square [19]. See the left panel of Fig. 4. We use 2D regular and Halton points as interpolation centers and polyharmonic kernel $r^4 \log r$ with polynomials of degree $m = 2$ as approximation space. The errors of standard and rational RBF interpolations are compared and the results are plotted in Fig. 4. As we observe, both standard and rational methods provide good approximations for this smooth function where the theoretical order $m + 1 = 3$ for the standard interpolation is (approximately) achieved for the rational interpolation as well. Since the function has a steep gradient, the obtained accuracy was predictable for the rational method but not necessarily for the standard one. The reason lies behind the localization through partition of unity which enriches the standard method for functions with steep gradients.

As another 2D example, we consider the Runge-like function

$$f(x, y) = \frac{1}{1 + b(x^2 + y^2)}, \quad (x, y) \in [-1, 1]^2, \tag{17}$$

for a constant $b \geq 25$. This function has a rational form with constant and degree two polynomials in its numerator and denominator, respectively. Thus, it should be recovered exactly if the rational RBF method be implemented with appended polynomials of degree at least 2. However, to see whether the Runge's phenomenon influences the rational RBF method, we plot on the left-hand side of Fig. 5 the errors when

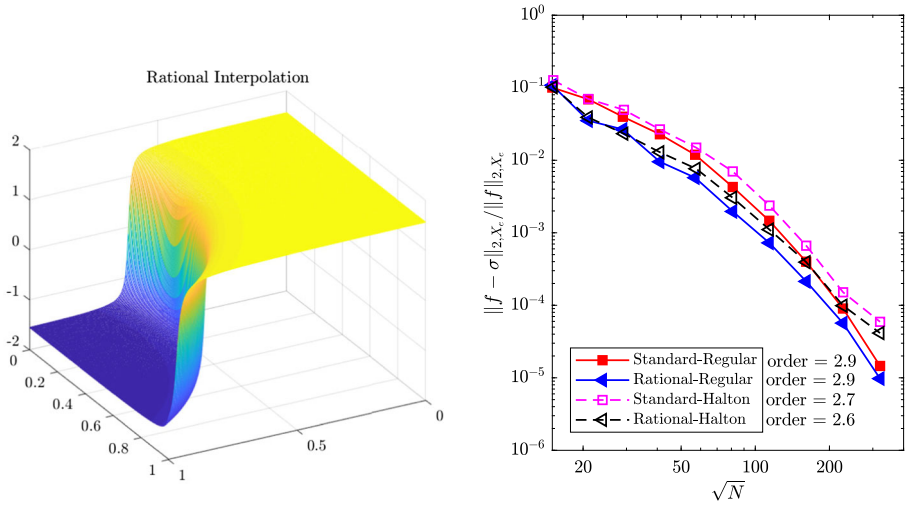

Fig. 4 The rational interpolation of the 2D function (16) on $N = 1681$ Halton points (left), and error plots for standard and rational RBF interpolations on different numbers of regular and Halton points (right). The polyharmonic spline $r^4 \log r$ with polynomials of degree $m = 2$ is used

$\varphi(r) = r^3$ and linear polynomials are employed. Halton points are used as interpolation points and results are obtained for different values $b = 25, 64$ and 100. The same results for the standard interpolation are given on the right-hand side of Fig. 5. As

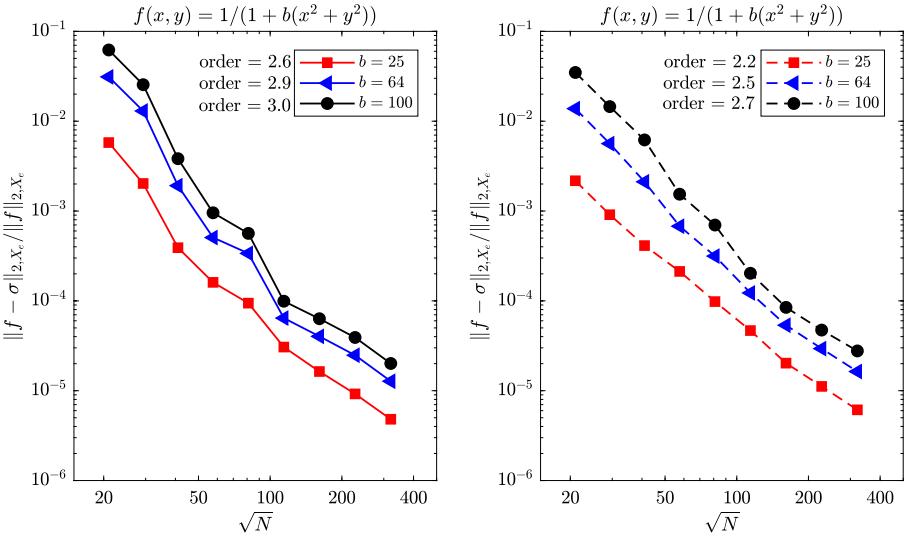

Fig. 5 Error plots for rational (left) and standard (right) RBF interpolations on Halton points for 2D function (17) with different values of parameter b. The polyharmonic spline r^3 with polynomials of degree $m = 1$ is used

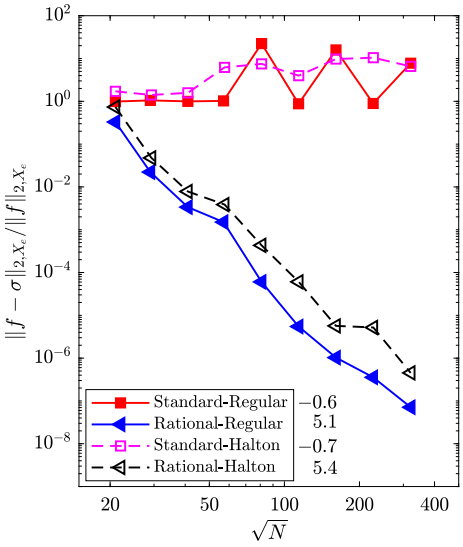

Fig. 6 Error plots of standard and rational RBF interpolations on regular and Halton points for 2D function (18). The polyharmonic spline $r^4 \log r$ with polynomials of degree $m = 2$ is used

similar to the previous example, both rational and standard methods produce accurate approximations for this smooth function. The use of low-order polynomials and localization via PU method avoid the Runge's phenomenon in both interpolants of this function.

For the last 2D example, we interpolate the function [8]

$$f(x, y) = \frac{\tan(9(y - x) + 1)}{\tan 9 + 1}, \quad (x, y) \in [0, 1]^2, \tag{18}$$

which has lots of singularities across six lines $y = x + ((k - 9/2)\pi - 1)/9$, $k = 1, \ldots, 6$. In Fig. 6, error plots of the standard and rational interpolations on regular and Halton points are illustrated. The rational interpolation approximates the function from its nodal values, excellently, while the standard one fails to give accurate results, as expected. This example again shows the superiority of the rational RBF method for singular functions. The surface plot of the rational interpolation on $N = 3314$ Halton points is depicted in Fig. 7.

Three dimensional examples were not covered in previous studies on rational RBF interpolation. In our last experiment, we consider the 3D singular function

$$f(x, y, z) = \frac{x}{\sin(\exp(0.5yz + 1))}, \quad (x, y, z) \in \Omega, \tag{19}$$

where Ω is a bumpy sphere defined in spherical coordinates via

$$\Omega := \{(r, \theta, \varphi) : r \leqslant R(\theta, \varphi),\ \theta \in [0, 2\pi),\ \varphi \in [0, \pi]\}, \tag{20}$$

where $R = \left[1 + \sin^2(2\sin\varphi\cos\theta)\sin^2(2\sin\varphi\sin\theta)\sin^2(2\cos\varphi)\right]^{1/2}$. We construct Halton and grid points on a smallest possible circumscribed cube and use their restrictions to Ω as interpolation points. Covering centers and evaluation points are produced, similarly. The shape of Ω and a set of Halton points are shown in Fig. 8. In Fig. 9 the relative errors on regular and Halton points for both rational and standard

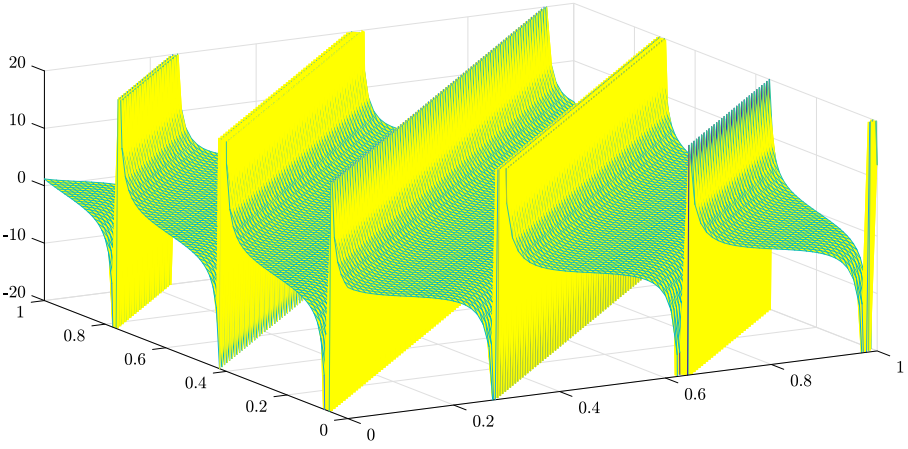

Fig. 7 The rational interpolation of the 2D function (18) on $N = 3314$ Halton points

interpolations are plotted. As we observe, the standard method fails to interpolate this singular function accurately while the rational method gives much more satisfactory results.

To observe the effect of scaling on stability of RBF systems we plot in Fig. 10 the minimum eigenvalue of the positive definite matrix $Z^T K Z$ in terms of $1/h$ on a patch with radius $\rho = 4h$ in 2D domain $[0, 1]^2$ and a patch with radius $\rho = 3h$ in 3D domain (20). As we pointed out, this matrix should be inverted to form the matrix S of generalized eigenvalue problem (8). In our situation, as h decreases the patch becomes localized more and more but the number of points remains approximately unchanged. However, [23, chap. 12] shows that the conditioning does not depend on the number of points but on their fill distance. The results are reported for the polyharmonic spline $r^4 \log r$ appended by polynomials of degree 2 with and

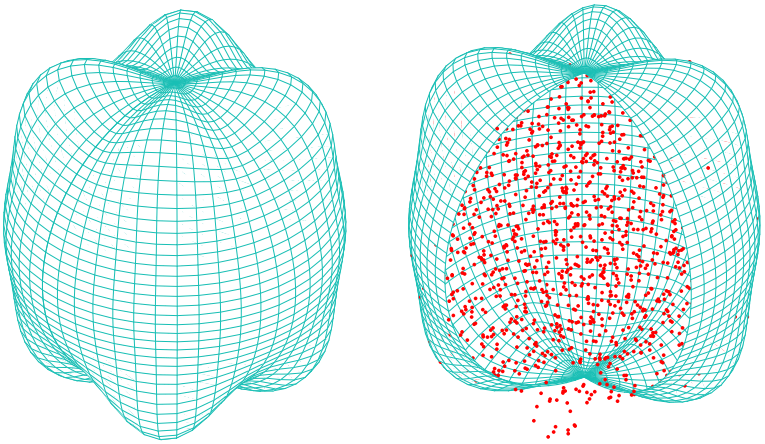

Fig. 8 A bumpy sphere (left), and a set of Halton points as interpolation centers (right)

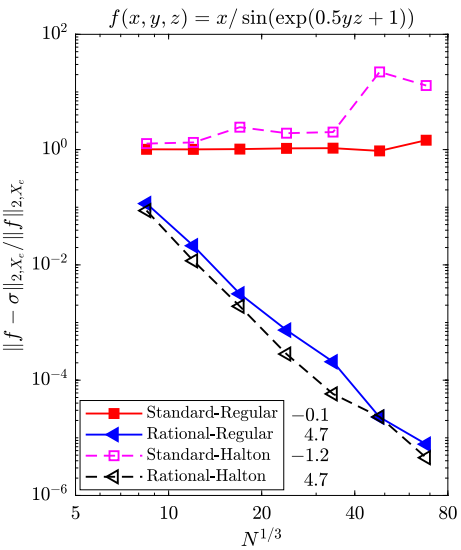

Fig. 9 Error plots for standard and rational RBF interpolations at different numbers of regular and Halton points for 3D function (19). The polyharmonic spline r^5 with polynomials of degree $m = 2$ is used

without scaling. For comparison, the results of the multiquadric function $\sqrt{1+(\varepsilon r)^2}$ with shape parameter $\varepsilon = 10$ are also included. This function is conditionally positive definite of order 1. Approximation with multiquadric kernel is not scalable. As we observe, the minimum eigenvalues remain approximately unchanged for the polyharmonic kernel when scaling is applied and approach zero otherwise. The worse behavior is observed for the multiquadric function even with this rather large shape

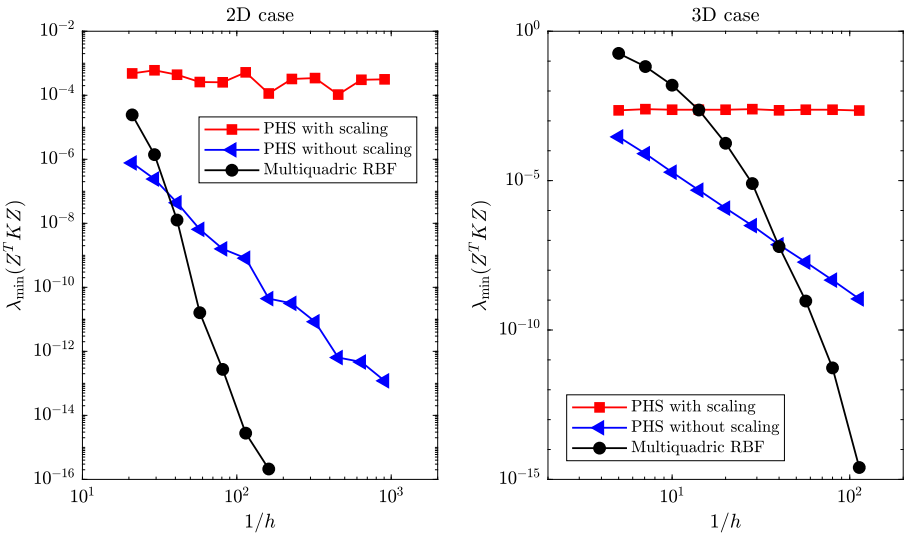

Fig. 10 The behavior of the minimum eigenvalue of matrix Z^TKZ on a local patch with radius $4h$ in 2D (left) and a local patch with radius $3h$ in 3D (right). The polyharmonic spline (PHS) $r^4 \log r$ with and without scaling, and the multiquadric function $\sqrt{1+100r^2}$ are used to construct the kernel matrix K

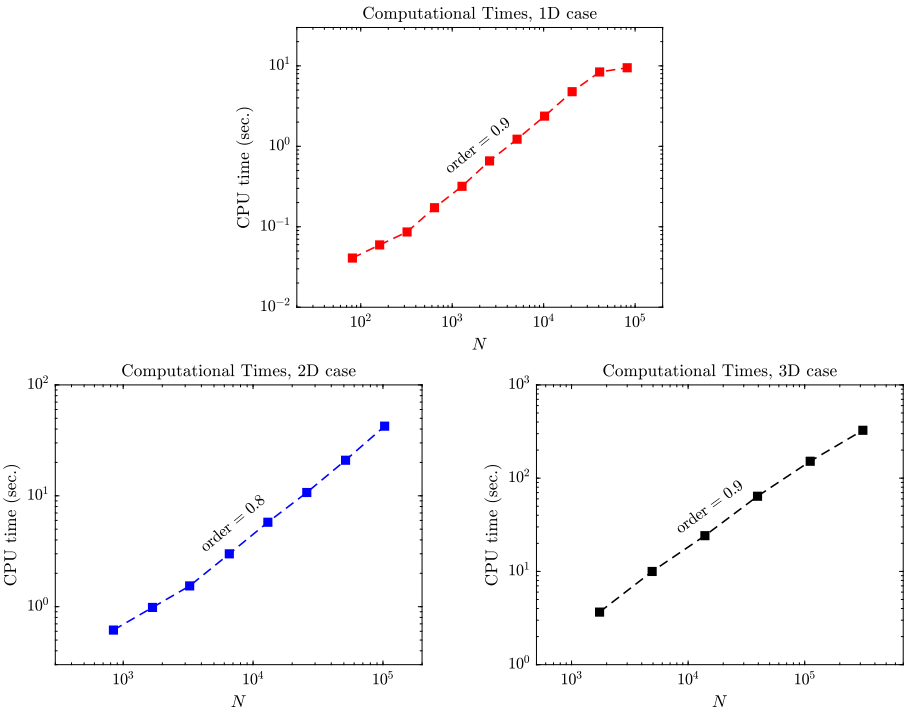

Fig. 11 Computational times v.s. N, the number of interpolation points in 1D, 2D and 3D problems. In all cases, a complexity near $\mathcal{O}(N)$ is observed

parameter. While not presented here, the conditioning of the saddle point matrix (5) obeys a same line in all cases.

Instabilities are also observed for other well-known kernels such as Gaussians and inverse multiquadrics which are not presented here. This is the main reason for us to focus on polyharmonic kernels in this paper. In [8] the idea of variably scaled kernels (VSK) [3] is used to avoid such instabilities for positive definite functions. More details about the conditioning of RBF matrices can be found in [23, chap. 12].

Finally, in Fig. 11 the plots of computational times with respect to N, the number of interpolation points, are shown for 1D, 2D, and 3D examples. In all cases, a complexity rate near $\mathcal{O}(N)$ is observed.

6 Conclusion

The rational RBF interpolation method was modified for conditionally positive definite kernels. A stable algorithm based on a scalable rational polyharmonic interpolation and the partition of unity method was developed. Some numerical experiments in one, two and three dimensions were given. Numerical results confirmed the robustness and accuracy of the new method. We leave studies on approximation of derivatives and other possible rational RBF techniques for a future work.

Acknowledgements We would like to thank the anonymous reviewers for their insightful comments which improved the quality of paper.

Funding The second author was in part supported by a Grant from IPM, No. 99650421.

References

1. Bayona, V.: An insight into RBF-FD approximations augmented with polynomials. Comput. Math. Appl. **77**, 2337–2353 (2019)
2. Benzi, M., Golub, G.H., Lieson, J.: Numerical solution of saddle point problems. Acta Numer., 1–137 (2005)
3. Bozzini, M., Lenarduzzi, L., Schaback R.M.: R.: Interpolation with variably scaled kernels. IMA J. Numer. Anal. **35**, 199–215 (2015)
4. Buhmann, M.D.: Radial Basis Functions: Theory and Implementations. Cambridge University Press, Cambridge (2004)
5. Buhmann, M.D., DeMarchi, S., Perracchione, E.: Analysis of a new class of rational RBF expansions. IMA J. Nume. Anal. **40**(3), 1972–1993 (2020)
6. Darani, M.R.A.: The RBF partition of unity method for solving the Klein-Gordon equation. Engineering with Computers In press (2020)
7. Davydov, O., Schaback, R.: Optimal stencils in Sobolev spaces. IMA J. Numer. Anal. **39**, 398–422 (2019)
8. De Marchi, S., Martínez, A., Perracchione, E.: Fast and stable rational RBF-based partition of unity interpolation. J. Comput. Appl. Math. **349**, 331–343 (2019)
9. Fasshauer, G.E.: Meshfree Approximations Methods with Matlab. World Scientific, Singapore (2007)
10. Gonnet, P., Pachòn, R., Trefethen, L.N.: Robust rational interpolation and least-squares. Elect. Trans. Numer. Anal. **38**, 146–167 (2011)
11. Iske, A.: On the approximation order and numerical stability of local Lagrange interpolation by polyharmonic splines. In: International Series of Numerical Mathematics, vol. 145, pp. 153–165. Birkhäuser Verlag (2003)
12. Iske, A.: On the construction of kernel-based adaptive particle methods in numerical flow simulation. In: Notes on Numerical Fluid Mechanics and Multidisciplinary Design (NNFM), pp. 197–221. Springer, Berlin (2013)
13. Jabalameli, M., Mirzaei, D.: A weak-form RBF-generated finite difference method. Comput. Math. Appl. **79**, 2624–2643 (2020)
14. Jakobsson, S., Andersson, B., Edelvik, F.: Rational radial basis function interpolation with applications to antenna design. J. Comput. Appl. Math. **233**, 889–904 (2009)
15. Larsson, E., Shcherbakov, V., Heryudono, A.: A least squares radial basis function partition of unity method for solving PDEs. SIAM J. Sci. Comput. **39**, A2538–A2563 (2017)
16. Mirzaei, D.: The direct radial basis function partition of unity (D-RBF-PU) method for solving PDEs. SIAM J. Sci. Comput. **43**, A54–A83 (2021)
17. Nakatsukasa, Y., Sète, O., Trefethen, L.N.: The AAA algorithm for ratinal approximation. SIAM J. Sci. Comput. **40**(3), A1494–A1522 (2018)
18. Safdari-Vaighani, A., Heryudono, A., Larsson, E.: A radial basis function partition of unity collocation method for convection—diffusion equations arising in financial applications. J. Sci. Comput. **64**(2), 341–367 (2015)
19. Scott, A.S., Bai, Y.: A rational radial basis function method for accurately resolving discontinuities and steep gradients. Appl. Numer. Math. **130**, 131–142 (2018)
20. Shepard, D.: A two-dimensional interpolation function for irregularly-spaced data. In: Proceedings of the 23th National Conference, pp. 517–523. ACM (1968)
21. Stoer, J., Bulirsch, R. Introduction to Numerical Analysis, 3rd edn. Springer, New York (2002)
22. Wendland, H.: Fast evaluation of radial basis functions: methods based on partition of unity. In: Approximation Theory, X: Wavelets, Splines, and Applications, pp. 473–483. Vanderbilt University Press, Nashville (2002)
23. Wendland, H.: Scattered Data Approximation. Cambridge University Press, Cambridge (2005)